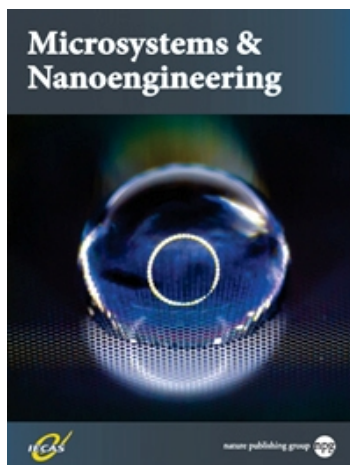


**Accepted Article Preview: Published ahead of advance
online publication**



**Fully Integrated Wearable Impedance Cytometry
Platform on Flexible Circuit Board with Online
Smartphone Readout**

Abbas Furniturewalla, Matthew Chan, Jianye Sui,

Karan Ahuja, Mehdi Javanmard

Abbas Furniturewalla, Matthew Chan, Jianye Sui, Karan Ahuja, Mehdi Javanmard. Fully Integrated Wearable Impedance Cytometry Platform on Flexible Circuit Board with Online Smartphone Readout. *Microsystems & Nanoengineering* accepted article preview 19 July 2018; doi: 10.1038/s41378-018-0019-0.

This is a PDF file of an unedited peer-reviewed manuscript that has been accepted for publication. NPG are providing this early version of the manuscript as a service to our customers. The manuscript will undergo copyediting, typesetting and a proof review before it is published in its final form. Please note that during the production process errors may be discovered which could affect the content, and all legal disclaimers apply.

Received 16 January 2018; accepted 9 May 2018

Fully Integrated Wearable Impedance Cytometry Platform on Flexible Circuit Board with Online Smartphone Readout

Abbas Furniturewalla, Matthew Chan, Jianye Sui, Karan Ahuja, Mehdi Javanmard
Department of Electrical and Computer Engineering, Rutgers, The State University of New Jersey, USA

Corresponding author: Mehdi Javanmard, [Email: mehdi.javanmard@rutgers.edu](mailto:mehdi.javanmard@rutgers.edu),

Abstract We present a wearable microfluidic impedance cytometer implemented on a flexible circuit wristband with on-line smartphone readout for portable biomarker counting and analysis. The platform contains a standard polydimethylsiloxane (PDMS) microfluidic channel integrated on the wristband, and the circuitry on the wristband composes of a custom analog lock-in amplification system, a microcontroller with an 8-bit analog to digital converter (ADC), and a Bluetooth module wirelessly paired with a smartphone. The lock-in amplification (LIA) system is implemented with a novel architecture which consists of the lock-in amplifier followed by a high-pass filter stage with DC offset subtraction, and a post-subtraction high gain stage enabling detection of particles as small as 1 μm using the 8-bit ADC. The Android smartphone application was used to initiate the system and for offline data-plotting and peak counting, and supports online data readout, analysis, and file management. The data is exportable to researchers and physicians for in-depth analysis and remote health monitoring. The system, including the microfluidic sensor, microcontroller, and Bluetooth module all fit on the wristband with a footprint of less than 80 cm^2 . We demonstrate the ability of the system to obtain generalized blood cell counts, however the system can be applied to a wide variety of biomarkers by interchanging the standard microfluidic channel with microfluidic channels designed for biomarker isolation.

Keywords: Microfluidics, Flow Cytometry, Impedance Spectroscopy, Lock-in Amplification, Remote Health Monitoring, Wearable Devices, Flexible Circuitry

1. Introduction

Increasingly capable smartphones and cheaper off-the-shelf components are constantly pushing what technology can achieve on-the-go¹. Robust and powerful electronics are driving progress for medical devices which can be chronically worn or implanted. With current capabilities of digital technology, data sharing, and cloud processing, scientists envision a virtual medical system for providing continuous patient-centered care remotely. Being able to monitor body health is crucial for early detection of illness, which in turn would allow for more accurate diagnosis, more efficient treatment, and lower morbidity or health repercussions².

However, there are tight budget constraints and medical criteria which biomedical devices must be approved for by the FDA to enter the market when considering wear-ability or implantability, such as weight and size, biocompatibility, aesthetic factors, and power consumption³. Many procedures have been performed in labs for decades with expensive and bulky equipment, which have yet to be translated to wearable health-monitoring technology. Nevertheless, the market for wearable devices has been rapidly growing due to recent achievements in developing miniaturized sensors⁴. For example, due to the development of incredibly robust and miniature accelerometers with microscale processing, devices such as the Fitbit have entered today's market for monitoring heart rate and user exercise activity⁵. In addition, a variety of flexible electronics are currently being developed by researchers to monitor perspiration for glucose levels and other biomarkers⁶⁻⁸. Flexible materials are suitable for wearable devices as they offer superior portability, durability, and robustness⁹.

In the laboratory setting, microfluidic procedures are commonly employed to gather biomedical information for purposes where only a few tens or hundreds of nanoliters of sample are to be analyzed. Macroscale biomedical systems may rely on sensors that lack precision regarding spatial access to or the size of the biological sample which can be analyzed, however microfluidic systems can be automated to routinely perform macromolecular separations of the target sample¹⁰. Lately, miniature microfluidic technologies, or "lab-on-a-chip" microfluidic systems are under investigation, as they have strong potential as wearable biosensors. A skin-like microfluidic device, for example, was recently developed to detect the pH, glucose, and lactate content in sweat through colorimetric sensing¹¹. In addition, microfluidics can be applied to create systems which can interface with the body in real time. For instance, a thread based toolkit of microfluidic sensors has been developed which can be embedded within body tissue, including a thread-based sensor developed for monitoring the pH of subcutaneous body fluids¹².

Flow cytometry is a specialized microfluidic research area where cells and biomarkers are purified through microfluidic separation, and particle counts are measured. Cell counting is an application of flow cytometry and can provide significant insight into a patient's health¹³. A well-known example includes a complete blood count (CBC) test which yields information about low or high red blood cell (RBC), white blood cell (WBC), or platelet levels amongst many other specific biomarker counts. However, there are limitations to how often blood counts can be obtained, especially because blood samples must be analyzed each time by a professional using expensive and bulky equipment only located in the laboratory setting. There is a need to achieve portable, user friendly systems to perform automated blood counts so that patient health can be continuously monitored outside of the lab without the need for professional intervention¹⁴.

Equipment for counting cells most commonly employs fluorescence-based spectroscopy or impedance spectroscopy (IS). Fluorescence-based cytometers require the fluorescent labeling of biological cells with markers

57 such as GHP. Continuous cell counting has been demonstrated *in vivo* using fluorescence-based flow cytometers¹⁵.
58 Unfortunately, existing optical instrumentation required to analyze fluorescent particles is overall bulky and
59 expensive, and the labeling procedure is tedious¹⁶. Coulter counting using IS¹⁷ is an alternative technique which
60 doesn't require the labeling procedure, and can be used to detect cells¹⁸, proteins¹⁹, and nucleic acids²⁰. The market
61 offers powerful and versatile coulter counters²¹ such as CytoFLEX (Beckman Coulter, Inc., Brea, CA, USA),
62 unfortunately these instruments also come in the form of costly and bulky benchtop equipment.

63 Alternatively, modern coulter counting has been demonstrated using inexpensive circuitry with miniaturized
64 footprints optimized for application-specific tasks such as blood cell-counting¹⁴. However, these cytometry systems
65 are not designed to be handled by a patient as they rely on expensive external data acquisition hardware and are not
66 packaged into a convenient, user-friendly, product. Furthermore, existing prototypes of portable cytometry systems
67 have been implemented on rigid circuit boards, which cannot be worn or implanted to allow continuous and
68 automated blood counting.

69 Moving away from expensive data acquisition hardware has been a challenge because microfluidic impedance
70 spectroscopy requires reading highly sensitive signals on the scale of nanovolts which fall below the noise level of
71 the environment. Lock-in amplification (LIA) is a method which is used to isolate such small signals, by using
72 phase-sensitive detection (PSD). A voltage at an elevated reference frequency is modulated with the impedance
73 response of the system, and the signal response is demodulated by mixing with the original excitation voltage and
74 applying a narrow band-pass filter around the reference frequency²².

75 Even through using lock-in amplification, the resulting signal's baseline may drift over an extended period,
76 reducing the amount of post-gain amplification which can be applied to the signal, and demanding the use of
77 powerful National Instrument data acquisition cards (National Instruments Corporation, Austin, Texas, USA) with
78 high-resolution (>16 bit) analog-to-digital converters (ADCs). However, in recent work²³ we developed a novel
79 analog LIA architecture, adding a baseline drift subtraction stage followed by a high-gain amplification stage to
80 allow a low-resolution (10-bit) ADC on a microcontroller unit (MCU) to sample the data (~1kHz frequency).
81 Although inexpensive MCUs with high-resolution ADC chips are on the market, more bits per sample poses new
82 challenges regarding processing performance and data transmission speeds. Therefore, using a low-resolution ADC
83 was preferable. The resulting system we developed was inexpensive, had a small footprint, and could accurately
84 detect impedance changes as small as .01%. We also used a Bluetooth module to transmit data between the
85 microcontroller and the smartphone, allowing the user to initiate data sampling and plot data results on the
86 smartphone. Although we achieved an easy-to-use user interface, our system still consisted of discrete components
87 and not packaged in a user-friendly manner to promote convenient usage outside of the lab.

88 In this work, we present a portable and fully integrated system including an LIA, a microfluidic
89 polydimethylsiloxane (PDMS) biosensor, a microcontroller, and a Bluetooth module all compacted onto a flexible
90 circuit board in the form of a low-profile wristband with live smartphone readout through an Android application.
91 Blood samples can be obtained via pin-prick and inserted into the inlet of the microfluidic channel for blood cell
92 counting. A medical professional can access the data remotely after being exported from the smartphone, or a
93 machine learning algorithm in the smartphone application could be used to alert the patient about the possibility of
94 illness.

95 Additionally, different biomarker counts can be obtained by interchanging different microfluidic devices which
96 isolate a specific cell type. For instance, if one wanted to use the platform to count neutrophil (a type of white blood
97 cell) to monitor for neutropenia (low neutrophil count), a high risk case for cancer patients undergoing
98 chemotherapy²⁴, the standard microfluidic PDMS chip used in this work can be replaced with a microfluidic device
99 for neutrophil purification²⁵.

100 An immediate benefit of the system being packaged as a wearable wrist-band is ultra-portability. A wearable
101 cell or particle quantifier could be utilized in a wide variety of biomedical and environmental applications. As an
102 example of important health applications, a catheter could be coupled to our system, and complete blood
103 cell counts (CBCs) could be obtained from patients on demand, similar to how temperature, blood pressure, and
104 pulse oximetry measurements can be currently readily obtained. This would especially be useful in an acute setting
105 for patients undergoing surgery or trauma care, where medical professionals need to make quick decisions based on
106 CBC results. Currently, large amounts of blood must be collected from patients and sent to a lab for analysis for
107 CBC counts. Instead, health workers in hospitals or on the field could wear a blood analyzer on their wrist and
108 move from patient to patient, performing rapid analysis. Ultimately, a wearable platform for continuous personal
109 health monitoring applications could also be envisioned if the pin-pricking mechanism is replaced with minimally
110 invasive microneedle or catheter-based impedance sensors which continuously sample venous blood without the
111 necessity for long intravenous tubes driven by bulky flow pumps. Doing so would have required extensive IRB
112 protocols and extensive resources for enrollment of patients and therefore was beyond the scope of this work.

113

114

115 In the context of environmental monitoring, a wearable impedance cytometer on the wristband could be utilized
 116 by inspectors and workers on the field, where different environments must be sampled for different particle counts,
 117 such as inorganic elements in mines, or bacteria and other contaminants in water samples. In difficult conditions
 118 where dexterity is reduced (in rivers, cold temperatures, etc.), a wearable device would be especially beneficial for
 119 performing quick analysis on-site as opposed to collecting and organizing samples and returning to the lab for
 120 analysis.

120

121

122

123

124

125

126

127

128

129

130

131

132

133

134

135

136

137

138

139

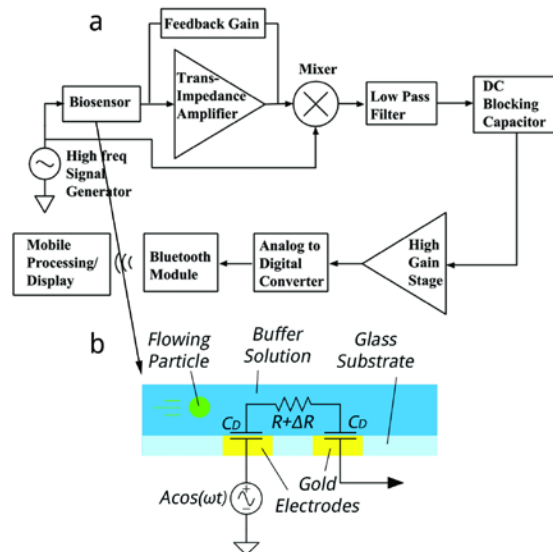
140

141

2. Materials and Methods

a. System Overview

The system diagram is displayed in Figure 1. We use our custom-built analog architecture²³, designed to detect highly sensitive impedance changes in a microfluidic channel with low-end hardware.



142

143

144

145

146

147

148

Figure 1. Custom-built analog architecture for impedance cytometry with off-the shelf hardware²³ a) System block diagram of cytometer-readout architecture b) Lateral view of microfluidic channel, where R represents channel resistance, ΔR is variable resistance from particle flow, and C_D is double-layer capacitance

To perform traditional lock-in amplification, a voltage at a high reference frequency is modulated with the microfluidic channel impedance, generating a current signal. The biosensor used in this work relies on an electric field generated between two electrodes within a microfluidic channel, with the baseline impedance representing

149 phosphate buffered solution (PBS), and variable impedance resulting from particle flow through the electric field. A
 150 trans-impedance amplifier then amplifies the input current signal and outputs a voltage signal, which is then mixed
 151 with the original reference voltage. Finally, a low-pass filter isolates the low frequency component of the product,
 152 which is a low-noise signal proportional to the channel impedance amplitude at the reference frequency²². As our
 153 channel impedance also varies with time, we designed the low-pass filter cutoff frequency to be larger than the
 154 inverse of the transit time of the microfluidic particle, or the time it takes for the particle to transverse the field
 155 between electrodes.

156 After performing traditional lock-in amplification on our biosensor, there remains a DC offset within the
 157 filtered signal which is in addition to our time-varying signal of interest. The DC offset limits the gain which can be
 158 applied to the signal before clipping occurs, and in²³, we describe the novel use of a DC blocking stage to subtract
 159 the offset and apply a post-subtraction high-gain amplification stage. The result is a highly sensitive architecture
 160 which can be implemented with a small footprint and off-the-shelf components. For an in-depth analysis on the
 161 architecture, including the noise analysis and simulation, we refer to the original work²³. An important note is that
 162 the DC blocking stage causes the positive voltage peak to be followed by a negative voltage peak with the same
 163 integrated energy, giving the novel architecture a uniquely shaped peak signature.

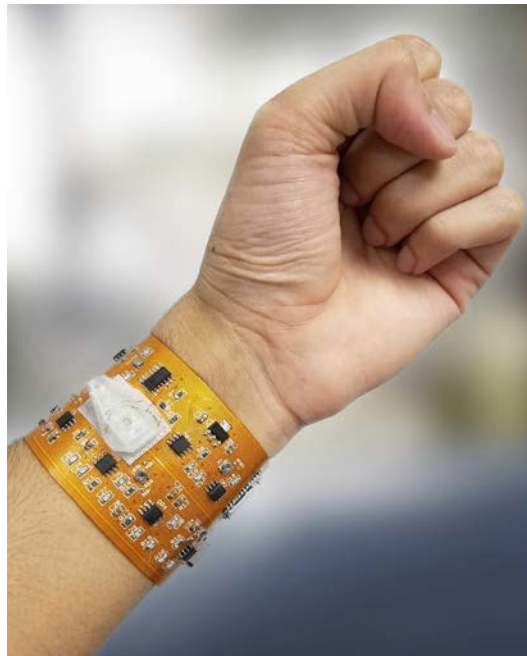
164 Because the analog signal has been amplified over several orders of magnitude, a low-end analog to digital
 165 converter (ADC) in a microcontroller chip can sample the data. The microcontroller interfaces with a Bluetooth
 166 module paired with a custom developed smartphone application. The application is used to initiate data sampling,
 167 and for data processing, readout, and analysis.

168

169 b. Flexible Circuit Description

170 We have implemented the architecture as a seamless and wearable microfluidic platform by designing a flexible
 171 circuit on a polyimide substrate in the form of a wristband (manufactured by FlexPCB, Santa Ana, CA, USA) as
 172 shown in Figure 2. All components, such as the batteries, microcontroller, Bluetooth module, and biochip are unified
 173 onto one board. The flexible circuit is a two-layer polyimide board with copper traces totaling an area of 8in².
 174 Surface-mount-packaged components were selected to compact the overall footprint and reduce noise.

175



176

177

178 *Figure 2. Wearable cytometry system on flexible PCB with integrated microfluidic PDMS chip, microcontroller, and*
 179 *BLE read out to smartphone (not shown)*

180 Lightweight coin cell lithium ion polymer (LIPO) batteries and regulator chips (LT1763 and LT1964 from
 181 Linear Technology) were used to provide $\pm 5V$ rails. A 1 MHz AC crystal oscillator (SG-210 from EPSON), D flip-
 182 flop (74LS74D from Texas Instruments) for frequency division, and passive LC tank was used to generate the 500-
 183 kHz sine wave 2 Volt Peak-to-Peak (V_{p-p}) signal, which is excited through the biosensor. The glass wafer acting as
 184 the substrate for the biosensor was cut around the PDMS slab with a diamond scribe to minimize the dimensions and

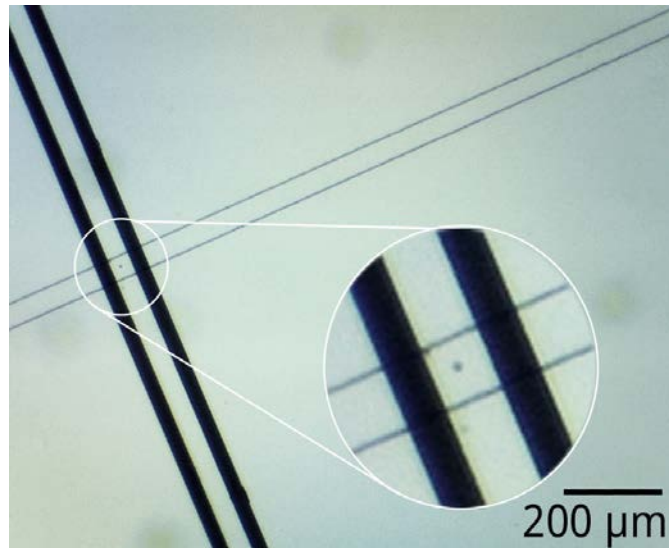
185 was attached to the board via micro-hook-tape and micro-loop-tape strips. The electrodes of the sensor interfaced
 186 with the board via jumping wires which were first soldered to the circuit's terminals and then bonded to the sensor's
 187 terminals with conductive epoxy. Removal of the PDMS sensor involves de-soldering the jumping wires from the
 188 circuit board, separation of the micro-hook strip adhered to PDMS sensor from the underlying micro-loop strip
 189 adhered to the board, and vice versa for the addition of another sensor. A DC-blocking capacitor was added prior to
 190 the biosensor to prevent low-frequency power surges from damaging the biosensor while the circuit was being
 191 switched on or off. The trans-impedance stage following the biosensor was implemented with a low noise
 192 operational amplifier (TL071CP from Texas Instruments) and a potentiometer in the feedback path for adjustable
 193 gain from .04 to .44. Mixing was achieved with a multiplier (AD835 from Analog Devices). To isolate the
 194 component of interest from the product of the mixing stage, a third order Butterworth low pass filter with a 100 Hz
 195 cutoff frequency and 60 dB roll off per decade was designed with another TL071CP op-amp²³. A DC-blocking
 196 capacitor was used for the DC blocking stage. The last stage of the analog design, the high gain stage, was achieved
 197 with two more TL071CP amplifiers. The first stage has a gain of 1000, and the second stage uses a potentiometer to
 198 adjust the gain between 100 and 1100. The high gain stage was minimized during the experiment for a net gain of
 199 10^5 .

200 An ATtiny 85 8-bit microcontroller from Atmel driven by an external 16 MHz on-board crystal was used to
 201 sample data. The microcontroller was programmed through the Arduino IDE (ARDUINO.CC) before being
 202 assembled on board. The HM-10 Bluetooth Low Energy (BLE) module was used for data transmission to the
 203 smartphone, with the module and the breakout circuit integrated on-board.

204 c. Biosensor Fabrication

205 The process used to micromachine our PDMS microfluidic channel for Coulter counting is a standard one
 206 and has been previously reported²⁷. We utilized channels with widths of 30 and 50 μm for our experiments, both 10
 207 μm high and 1 cm long. The aerial view of the 30 μm channel is shown in Figure 3.

208
209



210
211
212
213

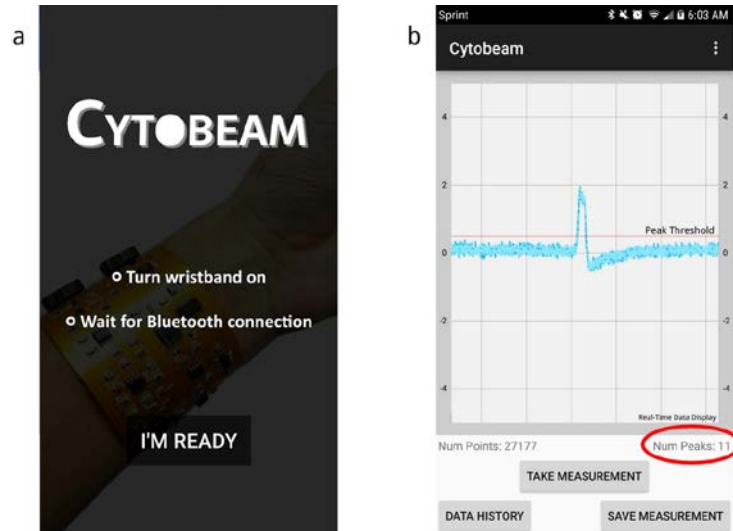
Figure 3. Top view of 30 μm microfluidic PDMS channel pore with sheep RBC shown flowing across electrodes

214 The electrode thicknesses we selected were 500 nm Cr followed by 100 nm Au. For the 50 μm channel, the
 215 electrode finger design consisted of 10 μm wide fingers separated by 15 μm . For the 30 μm channel, the width of the
 216 fingers was 20 μm separated by 30 μm . The PDMS is intrinsically hydrophobic preventing sufficient flow within the
 217 micro-channel²⁸. Poly(ethylene glycol)-based polymer containing dihydroxyphenylalanine and lysine (PEG-DOPA-
 218 K) was used to improve hydrophilicity and lubricity of the PDMS, improving particle flow²⁹.

219 d. Mobile Interface

220 We developed a Bluetooth Low Energy (BLE) based application developed for our platform designed to initiate data
 221 sampling from the analog circuit, save the data to storage, and plot the data post-sampling. In this work, we update
 222 the application to feature online data visualization and peak counting, as well as basic file management capabilities
 223 such as history data plotting and data exporting. Screenshots of the application are depicted in Figure 4. The

224 application update allows for the smartphone to serve as a replacement of the desktop software for the impedance
 225 spectrometer, optimized for the purposes of microfluidic particle counting. A specific advantage of online data
 226 readout which we take advantage of during experimentation includes the ability to simultaneously record optical
 227 microscopic results on a computer screen and the electronic data results on a smartphone screen with a 3rd party
 228 video recording device, making post-experimental analysis and data alignment more efficient.
 229



230
 231
 232 *Figure 4. Screenshots from our custom Android application of a) splash screen b) live data plot and peak count with*
 233 *buttons to initiate sampling, save the measurement, and plot history data*

234 e. Experimental Setup

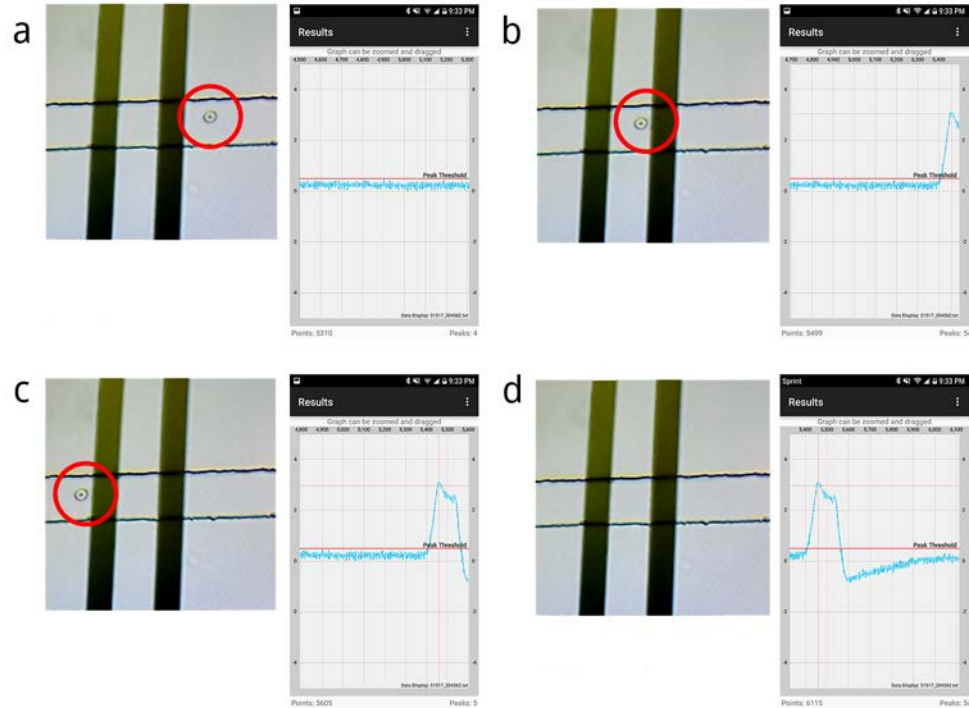
235 We used a minimalistic approach to circumvent traditional procedures requiring bulky and expensive
 236 equipment with newer procedures that can be performed outside of the lab. As mentioned before, the microfluidic
 237 PDMS channel was made hydrophilic by injecting a polyethylene glycol solution using a micropipette into the well
 238 of the channel, as opposed to traditional oxygen plasma treatment. Because the device was sufficiently hydrophilic,
 239 no external pump was required to generate a steady particle flow. If a specific blood cell type would like to be
 240 isolated, instead of using centrifugation (the standard lab approach), passive microfluidic geometries for blood cell
 241 sorting have been widely investigated³⁰, and can be integrated into microfluidic platforms as needed.

242 We tested our system with blank PBS, PBS with 3 μm polystyrene beads, sheep RBCs, and human blood
 243 cells (<10% WBCs and platelets, >90% RBCs). All samples were diluted in 10mM PBS with a dilution factor of 20
 244 to reduce to the likelihood of clogging in our simple microfluidic channel, and the channels were filled with 10mM,
 245 pH 7.4 phosphate buffered solution (PBS). A channel width of 50 μm was used when counting polystyrene beads
 246 and sheep blood cells, and a channel width of 30 μm was used when counting human blood cells obtained from
 247 finger pricks, corresponding to channel resistances of 12.5k Ω and 20.8 k Ω respectively.

248 To verify accuracy, an optical compound microscope was used alongside the digital readout system to
 249 verify the accuracy of the digitally reported particle counts. For the purposes of optical recording, the biosensor was
 250 removed from the surface of the board (while still connected to the system via the jumper cables) and was positioned
 251 under the microscope so that the sensor's electrodes were visible under the field of view as in Figure 3. A digital
 252 camera was mounted onto the microscope lens so that the channel flow could be monitored on the desktop screen.

253 Simultaneously, the lock in amplification system was turned on through a power switch. The Bluetooth
 254 module was paired with an Android smartphone running our custom Android application. Through the application,
 255 the microcontroller was prompted to begin sampling voltage data. The voltage data would then be plotted in live
 256 time on the smartphone application.

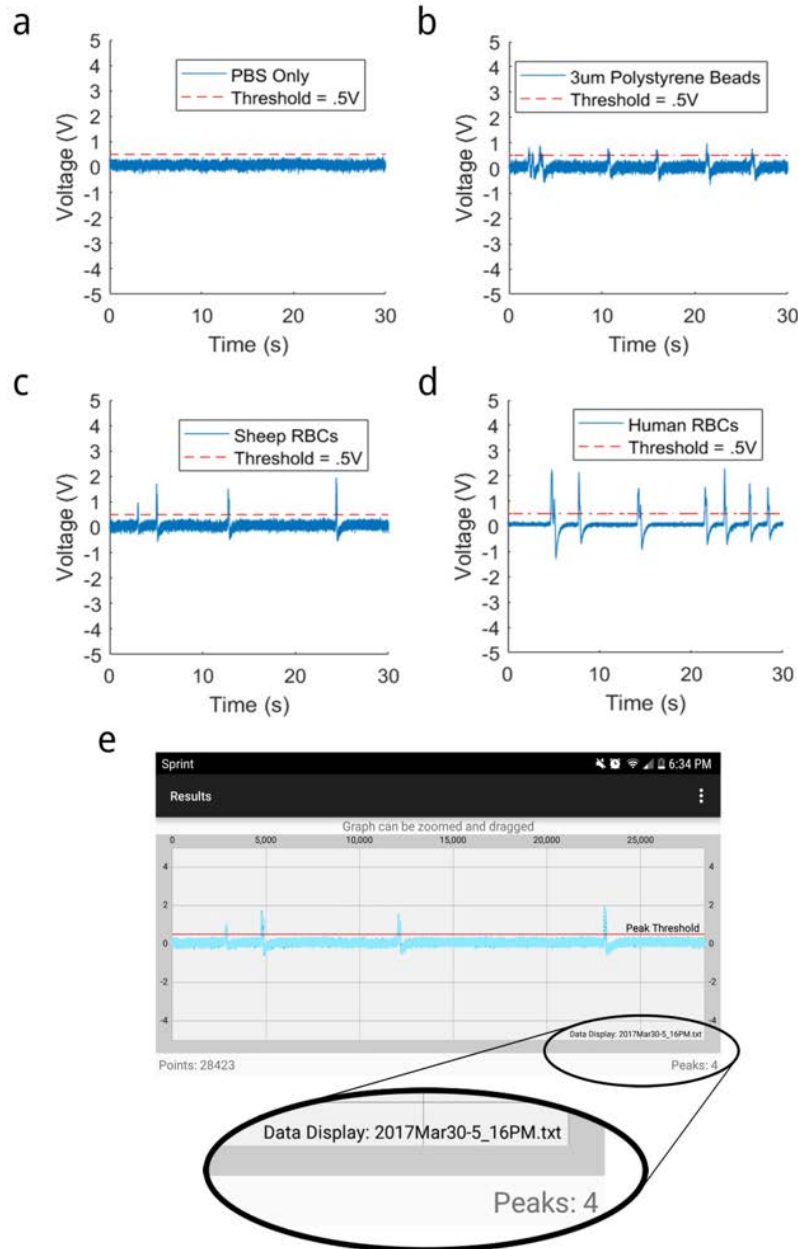
257 As the data was being sampled, a third-party device was used to video record the microscopic view on the
 258 desktop screen and the voltage signal on the smartphone, as shown in Figure 5.
 259



260
261
262
263 *Figure 5. Screenshots from video and cellphone recorded during experiment, combining the optical microscopic view*
264 *of the sensor and the digital data plotted on the smartphone as human RBC flows past the electrodes from a-d*

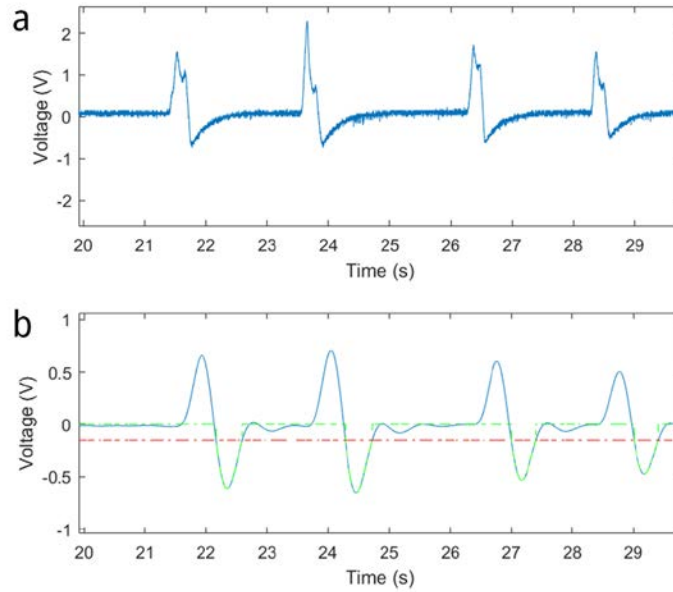
264 3. Results and Discussion

265 The results of 30 second experiments using blank PBS and PBS with 3 um polystyrene beads, sheep RBCs, and
266 human blood cells are displayed in Figure 6. Due to processing limitations of smartphone hardware, an efficient
267 algorithm was targeted to count the number of particles flowing through the channel in live time. Therefore, a
268 straightforward positive voltage threshold-based algorithm of .5V was used to count the number of peaks in the
269 smartphone. To remove false counts created by noise, we set a minimum quota in which four consecutive samples of
270 data were required to be above the threshold to iterate the peak count.



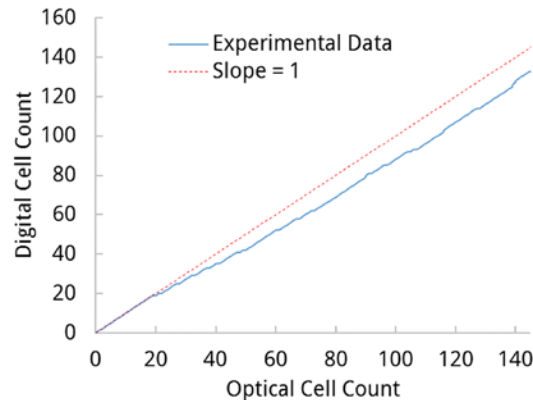
271
 272 *Figure 6. Data exported from smartphone application, measured through wearable LIA with PBS a) only b) and 3 μ m*
 273 *polystyrene beads c) and sheep blood cells flowing through 50 μ m PDMS channel d) and human blood cells flowing through*
 274 *30 μ m channel for 30 seconds. e) Results from figure (c) data shown on smartphone application*

275 For longer experimental samples, with large amounts of data, we performed post-experimental analysis in
 276 MATLAB R2016a (MathWorks Inc.) for peak counting. We ran an experiment with a duration of 10 minutes using
 277 human RBCs obtained via pin prick and diluted in PBS in a 30 μ m-wide channel. After the experiment, we exported
 278 the data file to a desktop computer. We envision that a patient would similarly export their data remotely to a
 279 physician for detailed analysis. The data file was opened in MATLAB and a Butterworth bandpass filter was applied
 280 using the Filter Designer from the MATLAB Signal Processing Toolbox. It was necessary to filter out the DC
 281 component of the signal to remove drift, and to filter out high frequencies to create a smooth signal, without
 282 significantly affecting signal amplitude. The resulting signal is shown in Figure 7. In the future, the application is
 283 envisioned to apply the low pass filter to the signal in live time.



284
285 *Figure 7. Selected data plotted to MATLAB from 10-minute experiment with human blood cells flowing through a 30*
286 *μm wide channel during an experiment with a duration of 10 minutes a) without modification b) after applying a Butterworth*
287 *band-pass filter using the Signal Processing Toolbox. The red dashed line represents the negative threshold voltage of -.2V, and*
288 *the green dashed line appears for peaks which included in the final count*

289 The negative voltage overshoot caused by the DC blocking capacitor helped identify peaks with a higher
290 accuracy than using the original positive voltage peak in the case that cells flow through the electrodes in proximity
291 to each other. Therefore, a negative threshold voltage was applied to count the peaks in MATLAB. The video
292 recording of the experiment was compared to the MATLAB results to analyze optical count versus digital count.
293 Representative is displayed in Figure 8.



294
295 *Figure 8. Total optical microscopic count vs. digital system count from 10-minute experiment with human blood cells*
296 Threshold-based automated counting only presented difficulty in identifying a peak when multiple cells
297 flowed between the electrodes at a given time resulting in the overlap of separate peaks. Each occurrence of
298 overlapping caused the digital to optical count ratio to drop. However, due to the unique peak signature from our
299 circuit response due to the DC blocking capacitor, we expect that multiple peak-fitting algorithms such as those used
300 in XPS analysis³¹ can be implemented to obtain more accurate counts.

302 4. Conclusion

303 We have developed a wearable microfluidic impedance cytometer on a flexible substrate containing a
304 microfluidic biosensor, analog readout hardware, an analog to digital data MCU, BLE transmission, and smartphone
305 data processing. Our platform can count the number of RBCs from a pin-prick blood sample pipetted into the
306 standard microfluidic PDMS chip. However, different types of biomarkers can be counted by replacing the standard
307 PDMS chip with specialized microfluidic chips that isolate a specific biomarker. Interchanging the biosensors on the
308 current version of the platform involves de-soldering and re-soldering jumping cables from the biosensor pads to the

board. The resulting voltage data can be exported and shared with a medical professional for in-depth analysis and can provide vital information to doctors without significantly disrupting a patient's daily schedule.

In future work, we aim to evaluate the robustness of our platform by sampling data as it is being worn, and we will adjust the circuit architecture, biosensor design, and overall packaging to reduce the effects of motion and environmental disturbance. In addition, we would like to demonstrate the versatility of the system by testing across a range of biosensors and biomarkers. Furthermore, studies will be dedicated to incorporating multi-frequency impedance spectroscopy and data-driven approaches to discriminate between different cell types. Lastly, our current system requires the user to place samples into the microfluidic channel obtained from a pin prick, which must be performed at intervals and as opposed to continuous and automated blood counting. Therefore, we envision fabricating minimally invasive microneedle or catheter-based impedance sensors continuously sampling venous blood using a wearable cytometry platform for readout. Bio-systems continuously monitoring human health is the key to early disease prediction and could revolutionize how medical professionals provide treatment to their patients.

Acknowledgements This work was partially funded by the National Science Foundation Instrumentation Development for Biological Research Grant award number 1556253. We would also like to thank John Scafidi and Steve Orbine at Rutgers University for their technical assistance.

Competing Interests The authors declare no conflict of interest.

Contributions AF designed the wristband, performed the experiments, and wrote the paper. MC updated the smartphone application for live data processing and readout. JS fabricated one of the microfluidic sensors and helped perform experiments. KA fabricated another one of the microfluidic sensors and helped perform experiments. MJ was the principal investigator of this work.

References

- Ozcan A. Mobile phones democratize and cultivate next-generation imaging, diagnostics and measurement tools. *Lab Chip* 2014; : 3187–3194.
- Shinbane JS, Saxon LA. Digital monitoring and care: Virtual medicine. *Trends Cardiovasc. Med.* 2016; **26**: 722–730.
- Pantelopoulou A, Bourbakis NG. A survey on wearable sensor-based systems for health monitoring and prognosis. *IEEE Trans. Syst. Man Cybern. Part C Appl. Rev.* 2010; **40**: 1–12.
- Markets MA. Portable Medical Devices Market Worth \$20 billion by 2018. 2013.
- Diaz KM, Krupka DJ, Chang MJ, Peacock J, Ma Y, Goldsmith J *et al.* Fitbit?: An accurate and reliable device for wireless physical activity tracking. *Int. J. Cardiol.* 2015; **185**: 138–140.
- Gao W, Emaminejad S, Nyein HYY, Challa S, Chen K, Peck A *et al.* Fully integrated wearable sensor arrays for multiplexed in situ perspiration analysis. *Nature* 2016; **529**: 509–514.
- Emaminejad S, Gao W, Wu E, Davies ZA, Yin Yin Nyein H, Challa S *et al.* Autonomous sweat extraction and analysis applied to cystic fibrosis and glucose monitoring using a fully integrated wearable platform. *Proc Natl Acad Sci* 2017; **114**: 201701740.
- Sempionatto JR, Nakagawa T, Pavinatto A, Mensah ST, Imani S, Mercier P *et al.* Eyeglasses based wireless electrolyte and metabolite sensor platform. *Lab Chip* 2017; **17**: 1834–1842.
- Kim D-H, Ghaffari R, Lu N, Rogers J a. Flexible and stretchable electronics for biointegrated devices. *Annu Rev Biomed Eng* 2012; **14**: 113–28.
- Mitchell P. Microfluidics — downsizing large-scale biology. *Nat Biotechnol* 2001; **19**: 717–721.
- Koh A, Kang D, Xue Y, Lee S, Pielak RM, Kim J *et al.* A soft, wearable microfluidic device for the capture, storage, and colorimetric sensing of sweat. *Sci Transl Med* 2016; **8**: 366ra165-366ra165.
- Mostafalu P, Akbari M, Alberti KA, Xu Q, Khademhosseini A, Sonkusale SR. A toolkit of thread-based microfluidics, sensors, and electronics for 3D tissue embedding for medical diagnostics. *Microsystems Nanoeng* 2016; **2**: 16039.
- Buttarelli M, Plebani M. Automated blood cell counts: State of the art. *Am J Clin Pathol* 2008; **130**: 104–116.
- Green R, Wachsmann-Hogiu S. Development, History, and Future of Automated Cell Counters. *Clin. Lab. Med.* 2015; **35**: 1–10.
- Pitsillides CM, Runnels JM, Spencer JA, Zhi L, Wu MX, Lin CP. Cell labeling approaches for fluorescence-

- 364 based in vivo flow cytometry. *Cytom. Part A*. 2011; **79 A**: 758–765.
- 365 16 Herzenberg LA, Parks D, Sahaf B, Perez O, Roederer M, Herzenberg LA. The history and future of the
366 Fluorescence Activated Cell Sorter and flow cytometry: A view from Stanford. In: *Clinical Chemistry*. 2002,
367 pp 1819–1827.
- 368 17 Cheung KC, Bernardino M Di, Schade-kampmann G, Hebeisen M. Microfluidic Impedance-Based Flow
369 Cytometry. 2010. doi:10.1002/cyto.a.20910.
- 370 18 Emaminejad S, Talebi S, Davis RW, Javanmard M. Multielectrode Sensing for Extraction of Signal from
371 Noise in Impedance Cytometry. *IEEE Sens J* 2015; **15**: 2715–2716.
- 372 19 Mok J, Mindrinos MN, Davis RW, Javanmard M. Digital microfluidic assay for protein detection. *Proc Natl
373 Acad Sci* 2014; **111**: 2110–2115.
- 374 20 Javanmard M, Davis RW. A microfluidic platform for electrical detection of DNA hybridization. In: *Sensors
375 and Actuators, B: Chemical*. 2011, pp 22–27.
- 376 21 Saleh OA, Sohn LL, Introduction I. Coulter counter. *Rev. Sci. Instrum.* 2001; **72**: 4449–4452.
- 377 22 Systems SR. About Lock-In Amplifiers, Application Note #3. 1999.
- 378 23 Talukder N, Furniturewalla A, Le T, Chan M, Hirday S, Cao X *et al*. A portable battery powered
379 microfluidic impedance cytometer with smartphone readout: towards personal health monitoring. *Biomed
380 Microdevices* 2017; **19**. doi:10.1007/s10544-017-0161-8.
- 381 24 Palmblad J, Nilsson CC, Höglund P, Papadaki HA. How we diagnose and treat neutropenia in adults. *Expert
382 Rev. Hematol.* 2016; **9**: 479–487.
- 383 25 Hou HW, Petchakup C, Tay HM, Tam ZY, Dalan R, Chew DEK *et al*. Rapid and label-free microfluidic
384 neutrophil purification and phenotyping in diabetes mellitus. *Sci Rep* 2016; **6**. doi:10.1038/srep29410.
- 385 26 Sasso L a, Aran K, Guan Y, Ündar A, Zahn JD. Continuous monitoring of inflammation biomarkers during
386 simulated cardiopulmonary bypass using a microfluidic immunoassay device - a pilot study. *Artif Organs*
387 2013; **37**: E9–E17.
- 388 27 Gawad S, Schild L, Renaud PH. Micromachined impedance spectroscopy flow cytometer for cell analysis
389 and particle sizing. *Lab Chip* 2001; **1**: 76–82.
- 390 28 Tan SH, Nguyen N, Chua C. Oxygen plasma treatment for reducing hydrophobicity of a sealed
391 polydimethylsiloxane microchannel. 2010; : 1–9.
- 392 29 Chawla K, Lee S, Lee BP, Dalsin JL, Messersmith PB, Spencer ND. A novel low-friction surface for
393 biomedical applications: Modification of poly(dimethylsiloxane) (PDMS) with polyethylene glycol (PEG)-
394 DOPA-lysine. *J Biomed Mater Res Part A* 2009; **90A**: 742–749.
- 395 30 Yu ZTF, Aw Yong KM, Fu J. Microfluidic blood cell sorting: Now and beyond. *Small*. 2014; **10**: 1687–
396 1703.
- 397 31 Axis K. Peak Fitting in XPS. *Casa XPS* 2006; : 1–29.
- 398
399
400
401
402
403
404
405